Turkish Journal of Electrical Engineering & Computer Sciences

http://journals.tubitak.gov.tr/elektrik/

Research Article

Turk J Elec Eng & Comp Sci
(2020) 28: 458 – 467

doi:10.3906/elk-1904-43

Controlling waveguide modes using $\mathcal{PT}$ transformation media

Hayrettin ODABAŞI*
Department of Electrical and Electronics Engineering, Faculty of Engineering, Eskişehir Osmangazi University, Eskişehir, Turkey

Received: 04.04.2019 • **Accepted/Published Online:** 07.08.2019 • **Final Version:** 27.01.2020

Abstract: We study rectangular waveguide modes loaded with parity-time ($\mathcal{PT}$) transformation media derived by complex transformation optics (CTO) approach. $\mathcal{PT}$ transformation media are obtained through mirror symmetric complex coordinate transformations resulting in a balanced loss/gain media. It is shown that waveguide modes can be controlled by simply changing the imaginary part of the complex coordinate transformation while not affecting any other characteristic of the waveguide. The field distribution inside the waveguide can either be stretched towards the sides or squeezed at the center of the waveguide by employing different loading configurations.

Key words: Complex transformation optics, waveguides, $\mathcal{PT}$ symmetry

1. Introduction

Transformation optics (TO) is a powerful technique that provides a systematic design methodology for the design of novel optical devices with new functionalities [1, 2]. Relying on the form invariance of Maxwell's equations, TO exploits the duality between the metric of the space and the constitutive parameters in Maxwell's equations [3, 4]. Combined with metamaterial technology, TO has enabled extreme topologies to be realized in laboratory environments, such as invisibility cloaks [5] and optical "black holes" [6–8], in addition to other designed devices [9].

Most TO applications rely on real-valued coordinate transformations implying that the derived material properties are supposed to be lossless. However, metamaterials are resonant structures and inherently lossy. Thus, TO-designed devices suffer from this associated unwanted loss [5]. Recently there has been an increased interest in complex transformation optics (CTO), where complex-valued coordinate transformations are performed to design novel devices [4, 8, 10–17]. With CTO, anisotropic loss/gain values can now be harnessed for useful purposes [8, 18]. In this case, the additional degrees of freedom and the ensuing material loss/gain enable new functionalities [8, 11–17] that are beyond the reach of conventional (real-valued) TO. In addition, because CTO-derived media are reflectionless, they can still perform the intended function even if the anisotropic loss/gain levels are high. In fact, spurious reflections are precisely one of the reasons why the addition of loss into real-valued TO-designed devices is so destructive. Perhaps the best-known example of CTO is that of perfectly matched layers (PML), commonly used in numerical simulations to truncate computational domains [19–21]. Although there are different formulations of PML, it was shown that PML can be derived as a result of complex coordinate transformation (or complex stretching) [4, 20, 22]. In addition, PMLs also serve as blueprints for

*Correspondence: hodabasi@ogu.edu.tr

physically realizable anisotropic absorbers [4, 21–23]. Another common use of CTO in electromagnetics is the formulation of complex source point (CSP) fields, where a point source is hypothetically placed at a complex location to obtain Gaussian beams in the paraxial regime [24–26]. Interestingly, it was shown that such an effect can also be realized via CTO [12–14], where Gaussian beams are generated via properly designed transformation media.

Waveguides are common components in many systems in areas of such as radar, communication, and imaging [27]. There is an increasing demand for waveguide structures with new capabilities. Although the basic characteristics of waveguides are enforced by their geometry, metamaterials have been extensively used for waveguides to obtain new features [28–35] (i.e. backward wave generation [28, 34], waveguide miniaturization [29, 35], and wakefield generation [31]). Transformation optics has also been applied to waveguide structures for different reasons [36–42]. It was shown that through TO, the waveguide modes can be preserved even in the presence of sharp corners and bends in addition to distortions on the surface of the waveguide [37–39, 42]. Furthermore, the waveguide cut-off frequencies can be controlled by using transformation media allowing miniaturization of waveguides [36, 40]. In addition, waveguide modes can be changed as desired by properly designing the coordinate transformation [40, 41].

In all of the above cases, the coordinate transformations were real-valued, resulting in real-valued material properties. In this paper, we study rectangular waveguide modes loaded with parity-time ($\mathcal{PT}$) transformation media derived from complex coordinate transformations. $\mathcal{PT}$ transformation media have been studied extensively in recent years due to their rich characteristics enabled by the combination of loss and gain media [12–17]. $\mathcal{PT}$ transformation media can be derived via mirror-symmetric complex coordinate transformation, resulting in balanced loss/gain media, i.e. $\epsilon(x) = \epsilon^*(-x)$. One important feature of the mirror-symmetric complex coordinate transformations is that there is no imaginary residual inside the waveguide in the transformed coordinate domain. As a result, the electrical thickness of the waveguide in the transformed coordinates is still real, i.e. the propagation constant is still real. We show that modes inside the waveguide can be controlled to either stretch or confine the mode profile by using two different loading configurations. With these mirror-symmetric transformations (if the real part of the complex stretching part is equal to 1), the cut-off frequency and the propagation constant remain unchanged while the field distribution is altered as desired. Since the media inside the waveguides are balanced loss/gain media, there is no net field decay or amplification in the propagation direction. Although not demonstrated here, by exploiting the real part (a_x) or imaginary part (σ_x) of the complex stretching parameter, one can control both the cut-off frequencies and mode distribution independently inside the waveguide.

2. Waveguide modes under complex coordinate transformations

Throughout the paper, we work in the frequency domain with the $e^{-i\omega t}$ convention. Now, consider a rectangular waveguide with PEC walls as depicted in Figure 1a. The waveguide has cross-section dimensions $a \times b$ and is loaded with a transformation medium with a total thickness of $2t$. Two different loading configurations are studied as shown in Figures 1b and 1c, respectively. We define a coordinate transformation from physical space (x, y, z) to an auxiliary space (x', y, z). The transformation for the side wall loading (Figure 1b) of the waveguide is given by

$$x' = \begin{cases} s_l x & \text{for} \quad 0 \le x \le t \\ x_1 + x - t & \text{for} \quad t \le x \le a - t \\ x_2 + s_g(x - (a - t)) & \text{for} \quad a - t \le x \le a, \end{cases} \tag{1}$$

where $x_1 = x'(t)$ and $x_2 = x'(a-t)$, where t is the thickness of the transformation region on each side. The transformation for the center loading (Figure 1c) of the waveguide is given as

$$x' = \begin{cases} x & \text{for} \quad 0 \le x \le t \\ s_l(x - (\frac{a}{2} - t)) + \frac{a}{2} - t & \text{for} \quad a/2 - t \le x \le a/2 \\ s_g(x - (\frac{a}{2} + t)) + \frac{a}{2} + t & \text{for} \quad a/2 \le x \le a/2 + t \\ x_3 + x - (\frac{a}{2} + t) & \text{for} \quad a - t \le x \le a, \end{cases} \tag{2}$$

where $x_3 = x'(\frac{a}{2} + t)$, $s_l = a_x + i\sigma_x$, and $s_g = a_x - i\sigma_x$ with $\sigma_x > 0$ being complex stretching parameters resulting in loss and gain media, respectively. Here, a_x and σ_x are the real and imaginary stretching parameters. Note that although similar transformations can be applied in other directions as well, we restrict ourselves to (x) transformation only. Both a_x and σ_x are functions of x only. Using TO, the effect of such coordinate transformation can be mimicked in physical space by material tensors (transformation media) $[\epsilon] = \epsilon_0 [\Lambda]$ and $[\mu] = \mu_0 [\Lambda]$ such that

$$[\Lambda] = \text{diag}\{1/s_x, s_x, s_x\}, \tag{3}$$

where $[\Lambda] = \det(S)^{-1} [S] [S]^T$ and S is the Jacobian of the transformation [1, 2, 4]. Note that outside of the transformation region the transformation medium recovers the free space, i.e. $[\Lambda] = 1$. The actual fields in physical space can be found from those in the transformed space [1, 2, 4] as

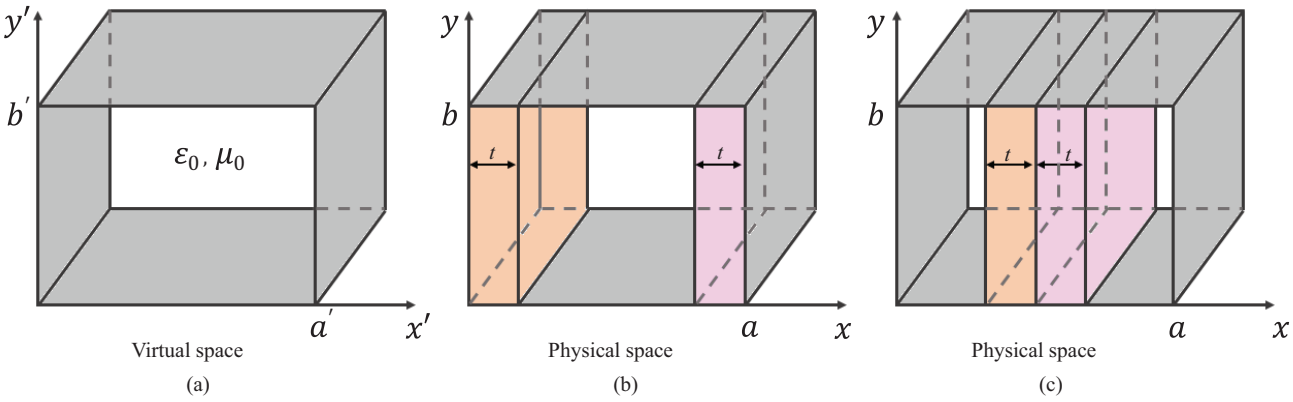

Figure 1. Cross-section of a rectangular waveguide in (a) transformed space, (b) physical space with transformation medium loaded on the side walls, and (c) physical space with transformation medium loaded at the center of the waveguide. The transformation region is shaded with two different colors to illustrate the $\mathcal{PT}$ transformation media such that one of them is loss medium and the other is gain medium, i.e. $\epsilon(x) = \epsilon * (-x)$.

$$\vec{E} = \left[S^{-1}\right]^T \cdot \vec{E}', \tag{4a}$$

$$\vec{H} = \left[S^{-1}\right]^T \cdot \vec{H}'. \tag{4b}$$

Now we need to derive the fields in transformed coordinates so that the real field in physical space can be obtained using Eq. (4). The fields in transformed coordinates can be found by applying an analytic continuation on coordinate x. The field solutions in the transformed space (with ϵ_0 and μ_0) for TE modes can be found as [27]

$$E'_x = \left(\frac{-i\omega\mu_0 k_y}{k^2 - k_z^2}\right) \cos(k_x x') \sin(k_y y)\, e^{ik_z z}, \tag{5a}$$

$$E'_y = \left(\frac{i\omega\mu_0 k_x}{k^2 - k_z^2}\right) \sin(k_x x') \cos(k_y y)\, e^{ik_z z}, \tag{5b}$$

$$E'_z = 0, \tag{5c}$$

and similarly for magnetic fields,

$$H'_x = \left(\frac{-ik_z k_x}{k^2 - k_z^2}\right) \sin(k_x x') \cos(k_y y)\, e^{ik_z z}, \tag{6a}$$

$$H'_y = \left(\frac{-ik_z k_y}{k^2 - k_z^2}\right) \cos(k_x x') \sin(k_y y)\, e^{ik_z z}, \tag{6b}$$

$$H'_z = \cos(k_x x') \cos(k_y y)\, e^{ik_z z}, \tag{6c}$$

with $k_x = m\pi/a'$, $k_y = n\pi/b$, $k_z = \sqrt{k^2 - k_x^2 + k_y^2}$, and $a' = x'(a)$, where m and n are the mode indices. Similar expressions can be written for TM modes and for the associated magnetic fields as well. For brevity, those expressions are not given here as we focus only on the dominant TE_{10} mode. Finally, the expressions for the real fields E_x, E_y, E_z in the rectangular waveguide with transformation media can be found by straightforward combination of Eq. (4), Eq. (5), and Eq. (6). The associated cut-off frequencies can also be obtained as

$$f_c = \frac{1}{2\pi\sqrt{\epsilon_0\mu_0}} \sqrt{k_x^2 + k_y^2}. \tag{7}$$

As can be seen from Eq. (7), the cut-off frequencies can be easily controlled by using the real stretching parameter a_x as a result of altered waveguide dimensions (a'). With the transformations given above, when $a_x = 1$ the cut-off frequency does not change for PT transformation media compared to the empty waveguide as the value of $a' = a$. However, if it were to be loaded with only a loss or gain medium there would be no cut-off frequency as the propagation constant becomes complex due to the now-complex waveguide length a'. For lossy media, small inclusion of loss will cause the waves to decay quickly before achieving any mode control. On the other hand, in gain media the field values will increase exponentially in the propagation direction. This case is interesting but difficult to implement as most gain media are nonlinear. As a result, the field amplitudes can quickly pass the gain saturation threshold and no mode control can be achieved. Therefore, we only focus on the mirror-symmetric coordinate transformation case in the following.

3. Results and discussion

In this section, we show analytical and numerical results for waveguides loaded with transformation media obtained by the complex transformation optics defined in Eq. (1)–(3). Numerical simulations are obtained using Comsol Multiphysics software. Note that such transformations are $\mathcal{PT}$-symmetric and the resulting media are balanced loss/gain media. In the following, we study two different loading configurations, each with different mode behaviors.

3.1. Side loading

Side loading of the transformation media is given in Figure 1b based on Eq. (1). The real-valued transformations have been studied before [40] and will not be pursued here. Instead, we show that one can achieve similar control over waveguide modes just by changing the imaginary part (σ_x) of the complex stretching factor. The real and imaginary parts of the complex coordinate x' are given in Figure 2a. As already mentioned, the real part is chosen as $a_x = 1$ while the imaginary part varies. Note that because the imaginary part switches signs in the second transformation region, the corresponding material comprises balanced loss/gain media. Thus, we have loss and gain media inside the waveguide simultaneously. The loss and gain media are depicted with different colors in Figure 2a for the corresponding increasing and decreasing profile of the imaginary profile of the transformed coordinate x'.

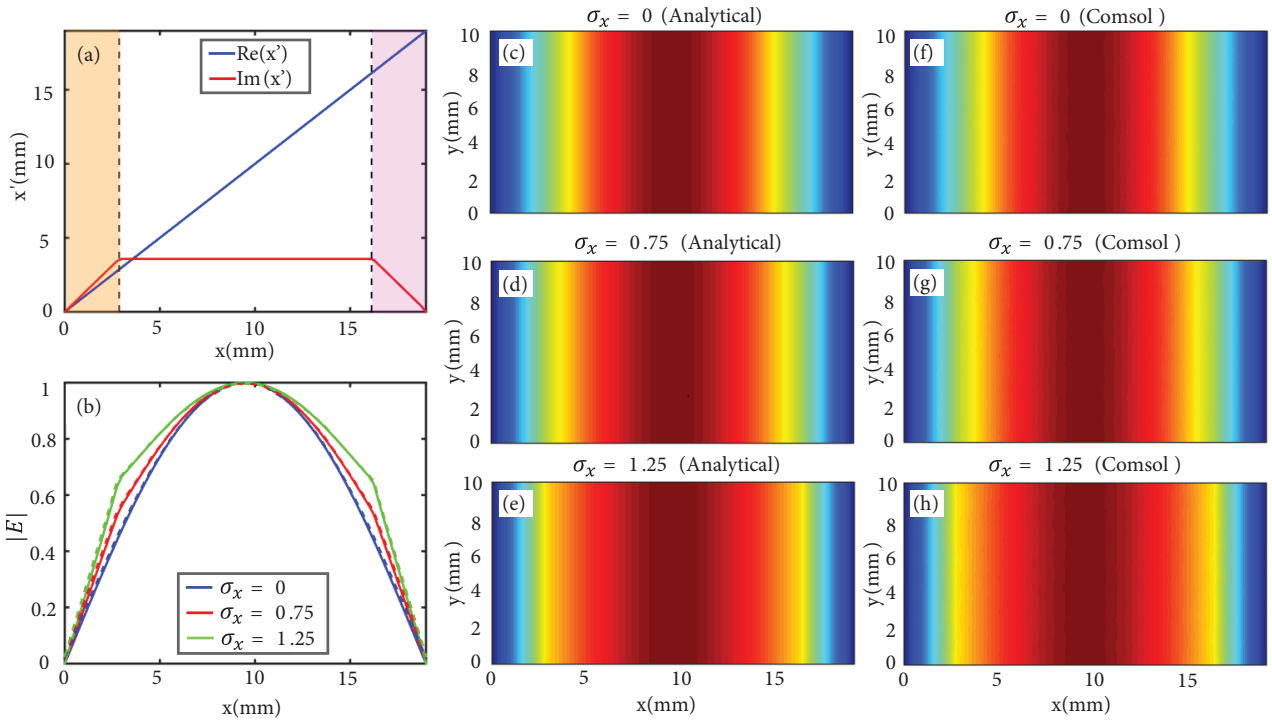

Figure 2. (a) The profile of the complex coordinate x' for the side loading of $\mathcal{PT}$ transformation media. The loss and gain region is depicted with different colors for the corresponding region. Here, $a_x = 1$ and $\sigma_x = 1.25$. (b) $|E|$ along the x direction ($y = b/2$) for the values of $\sigma_x = 0, 0.75, 1.25$ (Solid lines (analytical), dashed lines (numerical). (c–e) Analytical results of electric field magnitude ($|E|$) on a cross-section of the waveguide for each value of σ_x given above. (f–h) Numerical results for the cases in c–e.

Figure 2a shows the real and imaginary part of the transformed coordinate x' with respect to the original coordinate x. Figure 2b shows the magnitude of the electric field along the x direction (horizontal cut ($y = b/2$)) for various values of σ_x both for analytical and numerical results. Figures 2c–2e show the analytical results of the electric field distribution for different σ_x values on a cross-section. Note that the electric field distribution becomes more uniform inside the waveguide as σ_x increases, which can also be achieved by using only real transformations with $a_x > 1$ [37]. We would like to note that no optimization is done here to tune the values of transformation domain thickness and the σ_x values. Particularly, the σ_x values used here are to

demonstrate the effect of the approach rather then to provide the practical values for engineering purposes. It is beyond the scope of this paper to find the necessary parameters to get the best results. Figures 2f–2h show the numerical (Comsol) results of electric field distribution for same σ_x values. Excellent agreement is seen between the results.

3.2. Center loading

The profile of the transformation for center loading is given with Eq. (2) and depicted in Figure 3a. The first transformation region corresponds to loss media while the second region corresponds to gain media. The electric field along the x direction $(y = b/2)$ is given in Figure 3b for different values of σ_x for both analytical and numerical results. The corresponding electric field distribution on the cross-section for different σ_x values are shown in Figures 3c–3e for analytical and in Figure 3f–3h for numerical results, respectively. The effect of center loading is to focus the mode at the center of the waveguide unlike side loading. For both configurations one can have extreme control of mode by changing the complex stretching factor as well as the thickness of the transformation region.

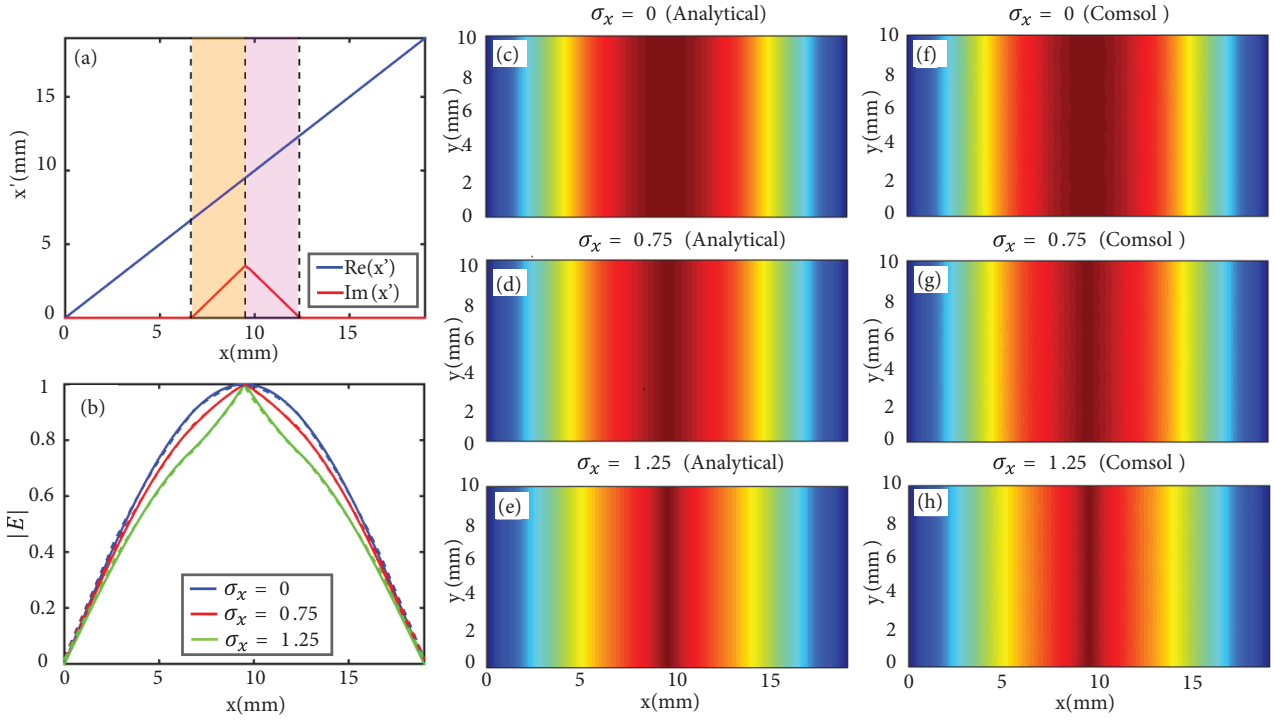

Figure 3. (a) The profile of the complex coordinate x' for the center loading of the $\mathcal{PT}$ transformation media. The loss and gain region is depicted with different colors for the corresponding region. Here, $a_x = 1$ and $\sigma_x = 1.25$. (b) $|E|$ along the x direction $(y = b/2)$ for the values of $\sigma_x = 0, 0.75, 1.25$ (Solid lines (analytical), dashed lines (numerical). (c–e) Analytical results of electric field magnitude ($|E|$) on a cross-section of the waveguide for each value of σ_x given above. (f–h) Numerical results for the cases in c–e.

Regardless of the configuration the field control can be enhanced by utilizing both the real (a_x) and imaginary (σ_x) part of the transformation. Depending on the application, either choice can be employed to get the desired output. Note that because the transformation medium derived here comprises balanced loss/gain

media, no net amplification or decay is realized in the propagation direction. As a result, such transformations allow one to control the mode behavior without changing any other waveguide characteristics. For instance, the real-valued transformations will change the cut-off frequency regardless of the nature of the transformation as long as $a' \neq a$ and $b' \neq b$. In that regard, CTO can provide independent control of the field distribution. Figure 4 shows numerical (COMSOL) results of the real part of the electric ($\Re e(E)$) and magnetic ($\Re e(H)$) fields of empty, side-loaded ($\sigma_x = 1.25$), and center-loaded ($\sigma_x = 1.25$) waveguides, respectively.

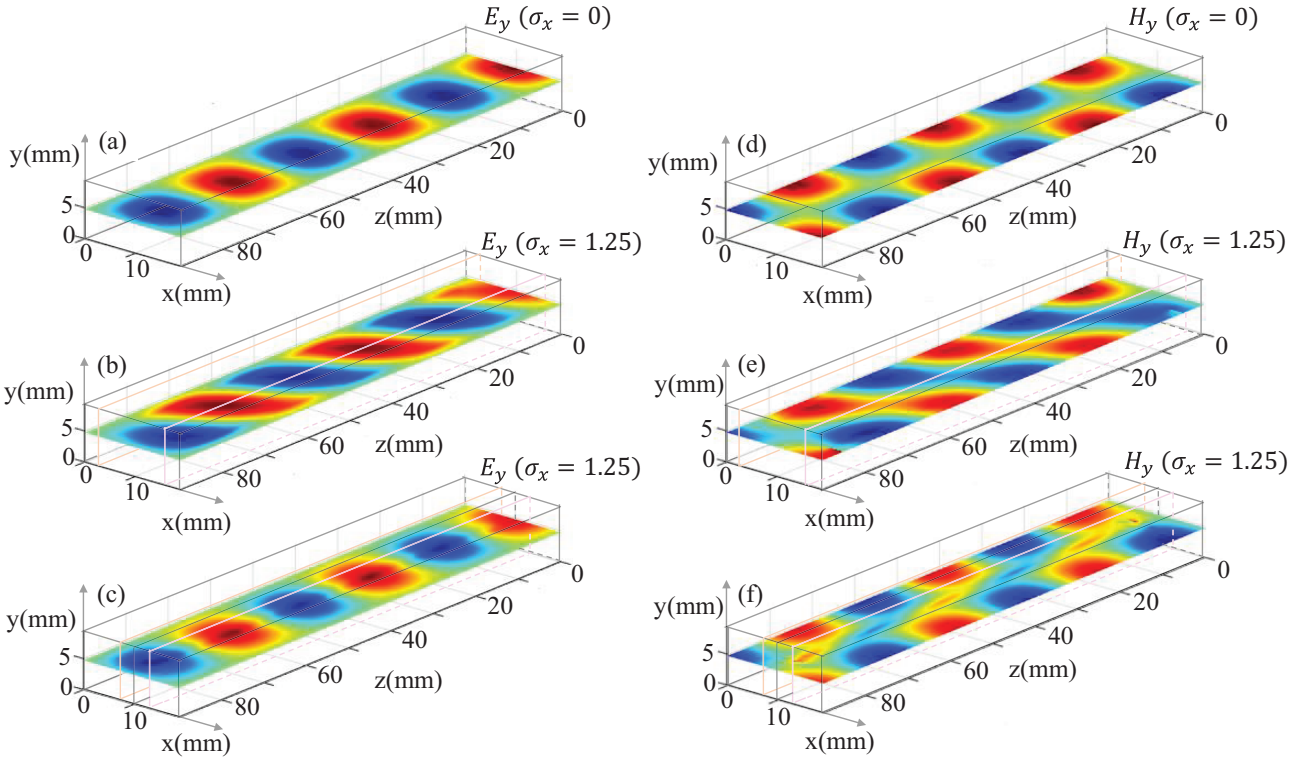

Figure 4. (a–c) Numerical results of electric field distribution inside (a) empty, (b) side-loaded, (c) center-loaded, respectively. (d–f) Same results for magnetic field. In this example, the imaginary part of the complex stretching parameter is chosen as $\sigma_x = 1.25$.

4. Conclusions and further remarks

We have studied rectangular waveguide modes under complex coordinate transformations. We have particularly focused on mirror-symmetric coordinate transformations, which yield $\mathcal{PT}$-symmetry, resulting in balanced loss/gain media. We have shown results for two different configurations based on the positions of the transformation media loadings. The actual fields inside the waveguide are derived using the TO approach. It is illustrated that the electric field distribution inside the waveguide can be made more uniform ('stretched') by placing the $\mathcal{PT}$ transformation media at the side walls of the waveguide. By increasing the imaginary part of the stretching parameter σ_x, the fields at the center of the waveguide can be made uniform in the extreme case. In the second configuration, we observed field focusing ('squeezing') more at the center of the waveguide in contrast to side loadings.

Contrary to real-valued transformations, with $\mathcal{PT}$-symmetric complex transformations the cut-off frequencies of the waveguide modes can remain unchanged. In addition, the propagation constant and other

waveguide properties do not change with $\mathcal{PT}$ transformation media. Thus, with $\mathcal{PT}$ transformation media, the field distribution can be controlled independently without affecting any other waveguide parameter unlike real-valued transformations [40].

It should be noted that no attempt is made here to optimize any parameter for particular performance criteria. Furthermore, it is assumed that we operate in a linear regime for gain media. Particularly, the values of σ_x used here are chosen to illustrate the effect of the approach as the realization of those materials tensors are subject to another study. With the advancement in metamaterial technology, such material tensors with both loss and gain characteristics can be realized over a finite frequency range [43–45].

References

[1] Pendry JB, Schurig D, Smith DR. Controlling electromagnetic fields. Science 2006; 312 (5781): 1780-1782. doi: 10.1126/science.1125907

[2] Leonhardt U. Optical conformal mapping. Science 2006; 312 (5781): 1777-1780. doi: 10.1126/science.1126493

[3] Ward AJ, Pendry JB. Refraction and geometry in Maxwell's equations. Journal of Modern Optics 1996; 43 (4): 773-793. doi: 10.1080/09500349608232782

[4] Teixeira FL, Chew WC. Differential forms, metrics, and the reflectionless absorption of electromagnetic waves. Journal of Electromagnetic Waves and Applications 1999; 13 (5): 665-686. doi: 10.1163/156939399X01104

[5] Schurig D, Mock JJ, Justice BJ, Cummer SA, Pendry JB et al. Metamaterial electromagnetic cloak at microwave frequencies. Science 2006; 314 (5801): 977-980. doi: 10.1126/science.1133628

[6] Narimanov EE, Kildishev AV. Optical black hole: broadband omnidirectional light absorber. Applied Physics Letters 2009; 95 (4): 9041106. doi: 10.1063/1.3184594

[7] Chen H, Miao RX, Li M. Transformation optics that mimics the system outside a Schwarzschild black hole. Optics Express 2010; 18 (14): 15183-15188. doi: 10.1364/OE.18.015183

[8] Odabasi H, Teixeira FL, Chew WC. Impedance-matched absorbers and optical pseudo black holes. Journal of the Optical Society of America B 2011; 28 (5): 1317-1323. doi: 10.1364/JOSAB.28.001317

[9] Jiang WX, Chin JY, Cui TJ. Anisotropic metamaterial devices. Materials Today 2009; 12 (12): 26-33. doi: 10.1016/S1369-7021(09)70314-1

[10] Kuzuoglu M. Analysis of perfectly matched double negative layers via complex coordinate transformations. IEEE Transactions on Antennas and Propagation 2006; 54 (12): 3695-3699. doi: 10.1109/TAP.2006.886489

[11] Popa BI, Cummer SA. Complex coordinates in transformation optics. Physical Review A 2011; 84 (6): 063837. doi: 10.1103/PhysRevA.84.063837

[12] Castaldi G, Savoia S, Galdi V, Alu A, Engheta N. $\mathcal{PT}$ metamaterials via complex coordinate transformation optics. Physical Review Letters 2013; 110 (17): 173901. doi: 10.1103/PhysRevLett.110.173901

[13] Savoia S, Castaldi G, Galdi V. Complex-coordinate non-Hermitian transformation optics. Journal of Optics 2016; 18 (4): 044027. doi: 10.1088/2040-8978/18/4/044027

[14] Odabasi H, Sainath K, Teixeira FL. Launching and controlling Gaussian beams from point sources via planar transformation optics. Physical Review B 2018; 97 (7): 075105. doi: 10.1103/PhysRevB.97.075105

[15] Fleury R, Sounas DL, Alu A. Negative refraction and planar focusing based on parity-time symmetric metasurfaces. Physical Review Letters 2014; 113: 023903.

[16] Alaeian H, Dionne JA. Parity-time-symmetric plasmonic metamaterials. Physical Review A 2014; 89: 033829.

[17] Odabasi H, Teixeira FL. Generalized Veselago-Pendry lenses via complex transformation optics. Optics Express 2019; 27:18 25670.

[18] Landy NI, Sajuyigbe S, Mock JJ, Smith DR, Padilla WJ. Perfect metamaterial absorber. Physical Review Letters 2008; 100 (20): 207402. doi: 10.1103/PhysRevLett.100.207402

[19] Berenger JP. A perfectly matched layer for the absorption of electromagnetic waves. Journal of Computational Physics 1994; 114 (2): 185-200. doi: 10.1006/jcph.1994.1159

[20] Chew WC, Weedon WH. A 3D perfectly matched medium for modified Maxwell's equations with stretched coordinates. Microwave and Optical Technology Letters 1994; 7 (13): 599-604. doi: 10.1002/mop.4650071304

[21] Sacks ZS, Kingsland DM, Lee R, Lee JF. A perfectly matched anisotropic absorber for use as an absorbing boundary condition. IEEE Transactions on Antennas and Propagation 1995; 43 (12): 1460-1463. doi: 10.1109/8.477075

[22] Teixeira FL, Chew WC. Systematic derivation of anisotropic PML absorbing media in cylindrical and spherical coordinates. IEEE Microwave and Guided Wave Letters 1997; 7 (11): 371-373. doi: 10.1109/75.641424

[23] Ziolkowski RW. The design of Maxwellian absorbers for numerical boundary conditions and for practical applications using engineered artificial materials. IEEE Transactions on Antennas and Propagation 1997; 45 (4): 656-671. doi: 10.1109/8.564092

[24] Keller JB, Streifer W. Complex rays with an application to Gaussian beams. Journal of the Optical Society of America 1971; 61 (1): 40-43. doi: 10.1364/JOSA.61.000040

[25] Deschamps GA. Gaussian beams as a bundle of complex rays. Electronics Letters 1971; 7 (23): 684-685. doi: 10.1049/el:19710467

[26] Felsen LB. Complex source point solution of the field equations and their relation to the propagation and scattering of the Gaussian beams. Symposia Matematica 1976; 18: 40-56.

[27] Pozar DM. Microwave Engineering (4th Edition). Hoboken, NJ, USA: John Wiley & Sons, 2011.

[28] Marqués R, Martel J, Mesa F, Medina F. Left-handed-media simulation and transmission of EM waves in subwavelength split-ring-resonator-loaded metallic waveguides. Physical Review Letters 2002; 89 (18): 183901. doi: 10.1103/PhysRevLett.89.183901

[29] Hrabar S, Bartolic J, Sipus Z. Waveguide miniaturization using uniaxial negative permeability metamaterial. IEEE Transactions on Antennas and Propagation 2005; 53 (1): 110-119. doi: 10.1109/TAP.2004.840503

[30] Belov PA, Simovski CR. Subwavelength metallic waveguides loaded by uniaxial resonant structures. Physical Review E 2005; 72 (3): 036618. doi: 10.1103/PhysRevE.72.036618

[31] Antipov S, Spentzouris L, Liu W, Gai W, Power JG. Wakefield generation in metamaterial-loaded waveguides. Journal of Applied Physics 2007; 102 (3): 034906. doi: 10.1063/1.2767640

[32] Edwards B, Alu A, Young ME, Silveirinha M, Engheta N. Experimental verification of epsilon-near-zero metamaterial coupling and energy squeezing using a microwave waveguide. Physical Review Letters 2008; 100 (3): 033903. doi: 10.1103/PhysRevLett.100.033903

[33] Dong YD, Yang T, Itoh T. Substrate integrated waveguide loaded by complementary split-ring resonator and its application to miniaturized waveguide filters. IEEE Transactions on Microwave Theory and Techniques 2009; 57 (9): 2211-2223. doi: 10.1109/TMTT.2009.2027156

[34] Meng FY, Wu Q, Erni D, Li LW. Controllable metamaterial-loaded waveguides supporting backward and forward waves. IEEE Transactions on Antennas and Propagation 2011; 59(9): 3400-3411. doi: 10.1109/TAP.2011.2161540

[35] Odabasi H, Teixeira FL. Electric-field-coupled resonators as metamaterial loadings for waveguide miniaturization. Journal of Applied Physics 2013; 114 (21): 214901. doi: 10.1063/1.4837597

[36] Ozgun O, Kuzuoglu M. Utilization of anisotropic metamaterial layers in waveguide miniaturization and transitions. IEEE Microwave and Wireless Components Letters 2007; 17 (11): 754-756. doi: 10.1109/LMWC.2007.908039

[37] Donderici B, Teixeira FL. Metamaterial blueprints for reflectionless waveguide bends. IEEE Microwave and Wireless Components Letters 2008; 18 (4): 233-235. doi: 10.1109/LMWC.2008.918869

[38] Huangfu J, Xi S, Kong F, Zhang J, Chen H et al. Application of coordinate transformation in bent waveguides. Journal of Applied Physics 2008; 104 (1): 014502. doi: 10.1063/1.2949272

[39] Roberts DA, Rahm M, Pendry JB, Smith DR. Transformation-optical design of sharp waveguide bends and corners. Journal of Applied Physics 2008; 93 (25): 251111. doi: 10.1063/1.3055604

[40] Teixeira FL, Odabasi H, Warnick KF. Anisotropic metamaterial blueprints for cladding control of waveguide modes. Journal of the Optical Society of America B 2010; 27 (8): 1603-1609. doi: 10.1364/JOSAB.27.001603

[41] Wang Z, Luo Y, Cui W, Ma W, Peng L et al. Controlling the field distribution in waveguides with transformation optics. Applied Physics Letters 2009; 94 (23): 234101. doi: 10.1063/1.3152004

[42] Ozgun O, Kuzuoglu M. Transformation electromagnetics based analysis of waveguides with random rough or periodic grooved surface. IEEE Transactions on Microwave Theory and Techniques 2013; 61 (2): 709-719. doi: 10.1109/TMTT.2012.2231428

[43] Sun L, Yang X, Gao J. Loss-compensated broadband epsilon-near-zero metamaterials with gain media. Applied Physics Letters 2013; 103 (20): 201109. doi: 10.1063/1.4831768

[44] Ye D, Wang Z, Xu K, Li H, Huangfu J et al. Ultrawideband dispersion control of a metamaterial surface for perfectly-matched-layer-like absorption. Physical Review Letters 2013; 111 (18): 187402. doi: 10.1103/PhysRevLett.111.187402

[45] Ye D, Chang K, Ran L, Xin H. Microwave gain medium with negative refractive index. Nature Communications 2014; 5: 5841. doi: 10.1038/ncomms6841